Protein thermodynamic destabilization in the assessment of pathogenicity of a variant of uncertain significance in cardiac myosin binding protein C

Maria Rosaria Pricolo[1,2,*], Elías Herrero-Galán[1], Cristina Mazzaccara[2,3], Maria Angela Losi[4], Jorge Alegre-Cebollada[1,*], Giulia Frisso[2,3]

[1] Centro Nacional de Investigaciones Cardiovasculares Carlos III (CNIC), Madrid, Spain
[2] Dipartimento di Medicina Molecolare e Biotecnologie Mediche. Università Federico II, Naples, Italy.
[3] CEINGE Biotecnologie Avanzate, scarl, Naples, Italy
[4] Dipartimento di Scienze Biomediche Avanzate, Università Federico II, Naples, Italy.

*To whom correspondence should be addressed: mrpricolo@cnic.es, jalegre@cnic.es

address of authors: elias.herrero@cnic.es; cristina.mazzaccara@unina.it; losi@unina.it; gfrisso@unina.it

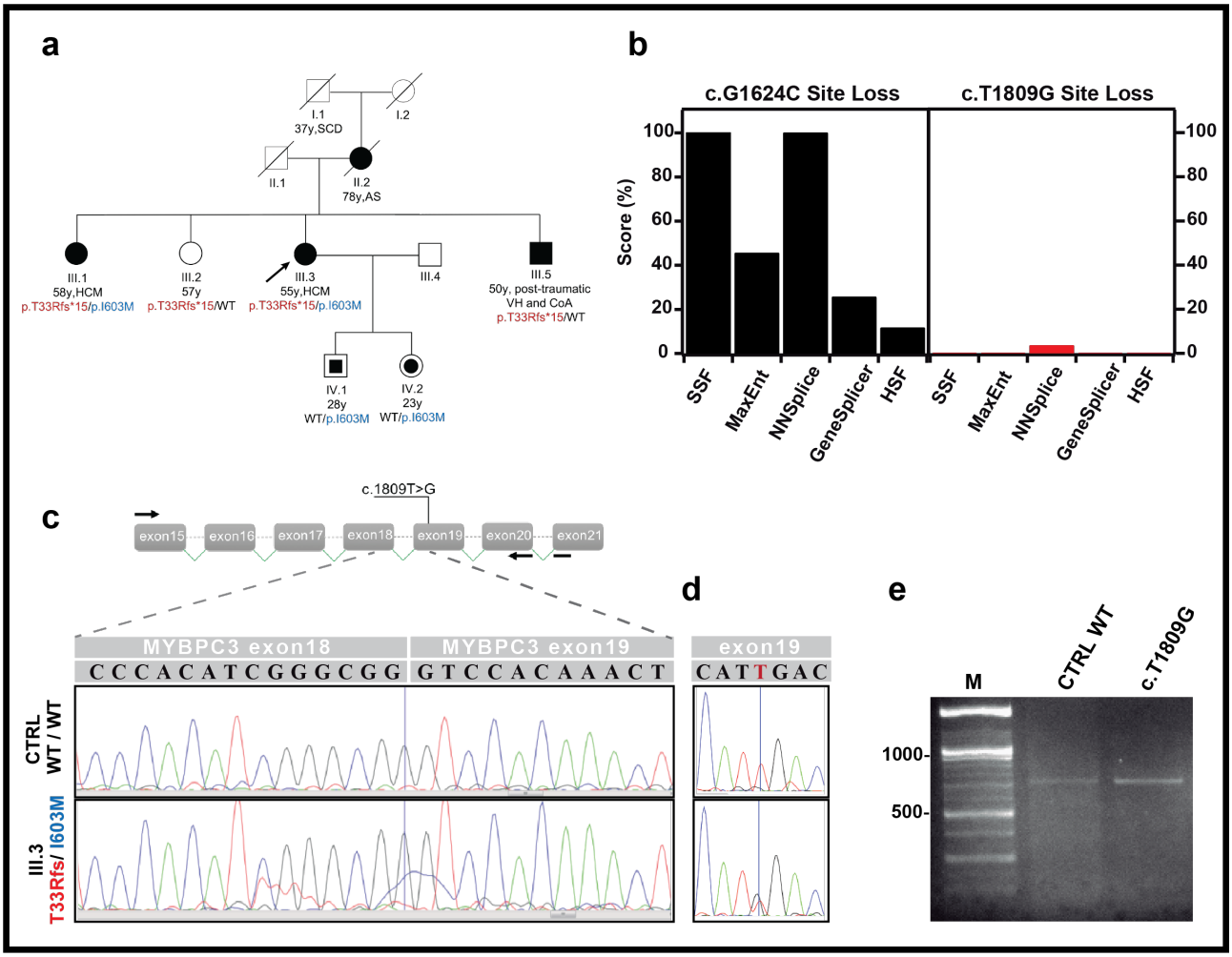

Figure 1: **Study of the potential effect of the MYBPC3-c.1809T>G (p.I603M) mutation on RNA splicing. (a)** Pedigree of four generations of the HCM family with the p.I603M variant. *Open symbols* represent subjects with a negative phenotype. *Filled symbols* represent clinically affected subjects. *Circles or squares with solid centres* indicate unaffected mutation carriers. Black arrow indicates the proband. Relevant clinical features are indicated: SCD, Sudden Cardiac Death; AS, Aortic Stenosis; HCM, Hypertrophic cardiomyopathy; VH, Ventricular Hypertrophy; CoA, coarctation of the Aorta. y:years. **(b)** Prediction of RNA splicing alterations using the Alamut software. Histograms represent the score given by the different prediction algorithms for a splicing site loss calculated between WT and the corresponding mutation. Evaluations were carried out with five

algorithms of splicing prediction: SSF (SpliceSiteFinder-like), MaxEnt, NNSPLICE (Neural Network Splice), GeneSplicer and HSF (Human Splicing Finder). Predictions for the c.1624G>C (E542Q) mutation (*left*). Prediction for c.1809 T>C (p.I603M) variant (*right*). For mutation c.1624G>C (E542Q), the loss of the canonical splicing site is detected by all the algorithms. For variant c.1809 T>C (p.I603M), the prediction suggests no RNA splicing alteration. (**c**) Experimental study of RNA splicing by RT-PCR analysis of mRNA isolated from peripheral blood. The MYBPC3 fragment analyzed is represented. Black arrows indicate forward and reverse PCR oligonucleotides. (**d**) Electropherograms obtained from cDNA sequencing of PCR fragments. CTRL WT corresponds to the analysis of mRNA obtained from a healthy, non-carrier subject. Electropherograms indicate the correct joining of exons 18-19 in both samples. The variant c.1809T>G is showed in heterozygosis in the electropherogram of patient. (**e**) Electrophoresis of RT-PCR analyses of mRNA. Lane 1: Marker XIV (Roche Diagnostics); Lane 2: Non-carrier control; Lane 3: c.1809T>G mutation. 1000, 500bp (units in the figure).

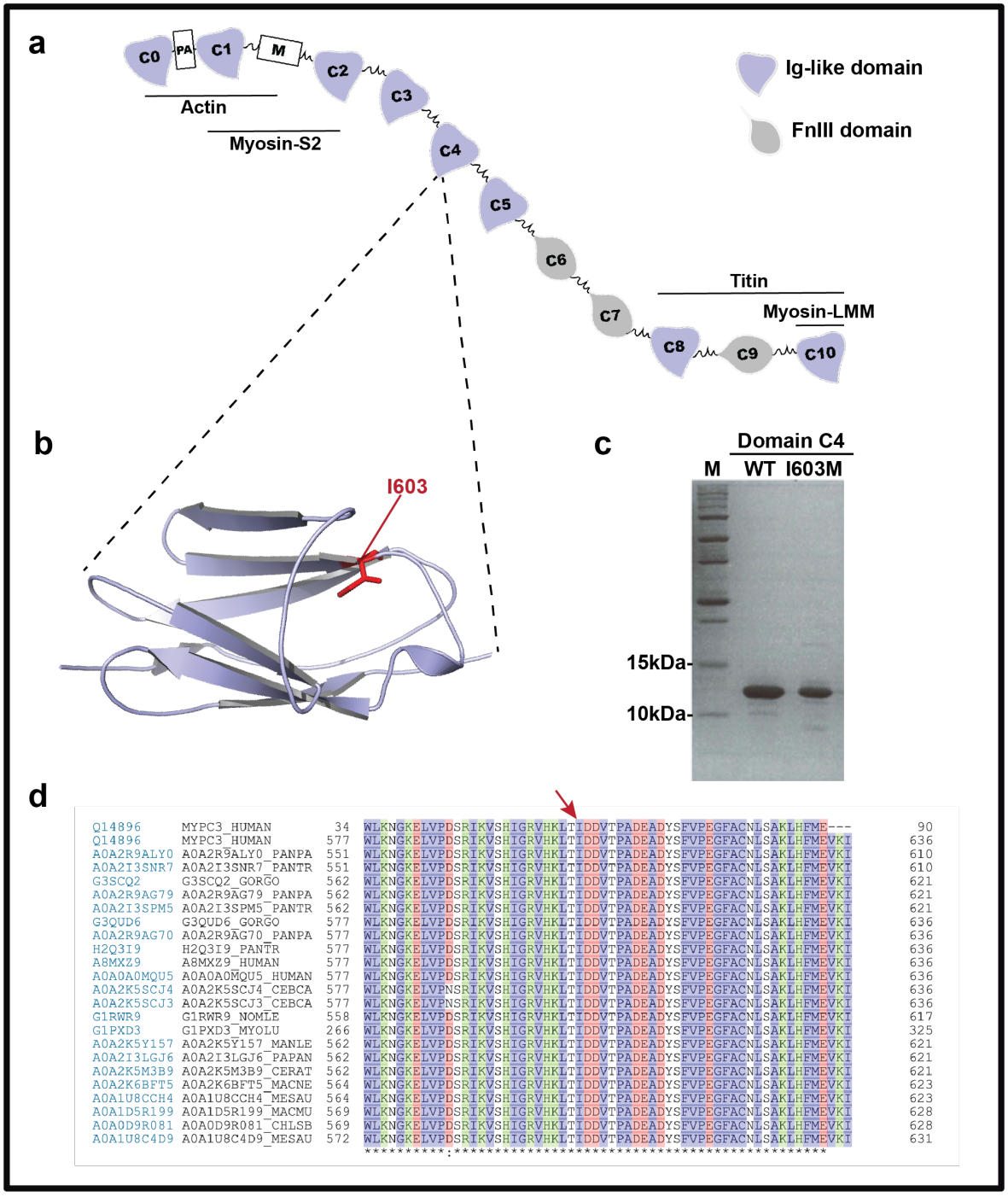

Figure 2: **MYBPC3-c.1809T>G (p.I603M) mutation at the protein level.** (**a**) Schematic representation of cardiac Myosin Binding Protein C (cMyBPC) and its sarcomeric interactors. cMyBPC is a multimodular protein composed by a series of immunoglobulin-like (*violet*) and fibronectin-type III (*gray*) domains. PA correspond to Pro/Ala rich region between C0 and C1. A 105-residue linker between C1 and C2 is called M-motif (M). The NH_2-terminus of cMyBPC interacts with Actin (C0-M) and the myosin-S2 domain (C1-M-C2). The COOH-terminus of cMyBPC interacts with titin (C8-C10) and light meromyosin (C10). (**b**) Homology modelling prediction of cMyBPC C4 domain. Graphic representation of the 3D structure of C4 WT domain, modelled with I-tasser using slow-MyBPC as a template (2YUZ PDB structure). The position of the isoleucine replaced in HCM patients is shown in red. The models of C4 domain have been prepared with PyMOL. (**c**) SDS-PAGE analysis of purified recombinant C4 domain expressed in *E. coli* BLR21 (DE3). (**d**) Sequence alignment of human cMyBPC C4 domain with other species. Data from UNIPROT were aligned by ClustalW. Regions between amino acids 34-87 of C4 domain are shown. The red arrow indicates the position of Ile 603.

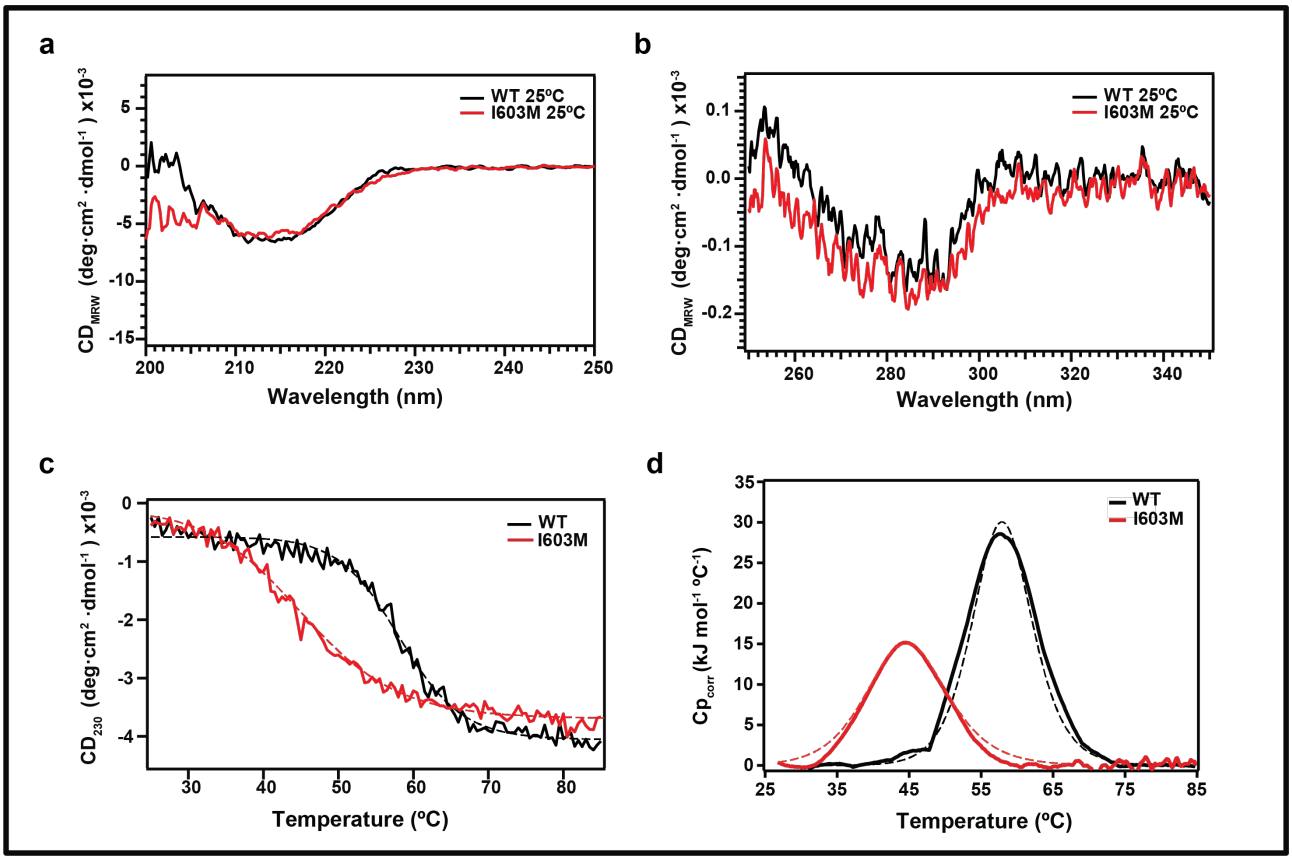

Figure 3: **The I603M mutation leads to thermodynamic destabilization of the C4 domain of cMyBPC.** (**a**) Far-UV CD spectra of native cMyBPC C4 WT (*black*) and I603M (*red*) monitored at 25°C. (**b**) Near-UV CD spectra of native C4 WT (*black*) and C4 I603M (*red*). (**c**) Thermal denaturation curves obtained for C4 WT (*black*) and I603M (*red*) by tracking CD signal at 230 nm as a function of temperature. The temperature at the midpoint of the transition, T_m is obtained by performing a sigmoidal fitting to denaturation curves (*dashed lines*) considering a two-state unfolding process. C4 WT domain shows a T_m of 58°C, 13°C higher than C4 I603M. (**d**) Thermal unfolding of C4 WT and C4 I603M monitored by DSC. Thermograms represent processed experimental data after baseline subtraction. The calorimetric enthalpy was calculated by integration of the area under the thermogram peak. The van't Hoff enthalpy was determined by fitting to a two-state model of unfolding (*dashed lines*).